## ChemComm



## COMMUNICATION

**View Article Online** 



Cite this: Chem. Commun., 2015 51 14111

Received 6th June 2015, Accepted 5th August 2015

DOI: 10.1039/c5cc04678e

www.rsc.org/chemcomm

## Electronically addressable nanomechanical switching of i-motif DNA origami assembled on basal plane HOPG†

R. Campos, ab S. Zhang, ab J. M. Majikes, L. C. C. Ferraz, T. H. LaBean, C M. D. Dongab and E. E. Ferapontova\*ab

Here, a pH-induced nanomechanical switching of i-motif structures incorporated into DNA origami bound onto cysteamine-modified basal plane HOPG was electronically addressed, demonstrating for the first time the electrochemical read-out of the nanomechanics of DNA origami. This paves the way for construction of electrode-integrated bioelectronic nanodevices exploiting DNA origami patterns on conductive supports.

Development of complex 2D and 3D DNA self-assembling nanostructures has enabled a new-generation of biomedically and bioelectronically useful nanomaterials for DNA-based nanolithography,1 targeted drug delivery systems,2 and nanomachines and nanorobots operating as biological sensor and actuator systems.3-6 Most of the latter systems are demonstrated to be highly efficient in solution. However, the current practical vision rather aims at solid-state supported nanomachinery devices possessing a broad spectrum of activating and sensing properties.8 The most challenging is adaptation of nanomachines and nanorobots for operation within the electronically addressable formats that allow large-scale manufacturing of highly efficient and cost effective functional materials miniaturised below the microelectronic chip size.9 Therewith, conductive supports used for interfacing the operating DNA nanodevices and electronics can dramatically affect and even interfere with the nanodevice mechanics, 10,111 putting in focus the "know-how" strategies for conservation of nanodevice biorecognition and nano-mechanical features in functional bioelectronics.

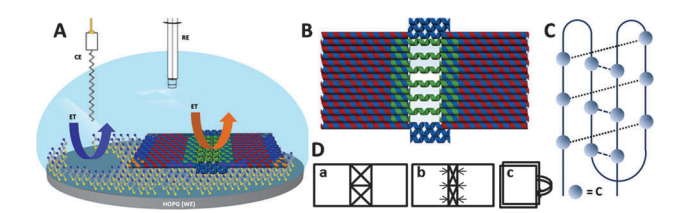


Fig. 1 Schematic representation of the (A) electrochemical set up used for AFM and electrochemical characterization of DNA origami on basal plane HOPG; (B) origami structure containing the pH-sensitive i-motif in its centre (the image was generated by caDNAno, the scaffold is in blue and staples are in red; the i-motif staples are in green); (C) a typical i-motif quadruplex structure formed in acidic solutions; and (D) possible conformational states of the origami B at (a) pH 8 and (b and d) below pH 5; (a) open-book state, (b) i-motif compact cleft state; and (c) closed book state.

Here, we aimed at electronically responsive pH-induced nanomechanical switching of the DNA origami<sup>12</sup> nanostructure self-assembled on conductive and atomically flat basal plane HOPG (highly ordered pyrolytic graphite) surface (Fig. 1A). The DNA origami studied here (and described in detail elsewhere)<sup>13,14</sup> is rectangular with dimensions of 60 nm by 32 nm, with a pH-sensitive i-motif composed of cytosine rich repeating sequences in its central part (Fig. 1B and Table S1 and Fig. S1, ESI†). Under acidic conditions (pH 4-5) these sequences are known to form a four-stranded structure held together by hemiprotonated (C°C<sup>†</sup>) base pairs and intercalated inter-strand interactions (Fig. 1C). 15-17 In basic solutions the designed origami should adopt an "open book" configuration that undergoes certain conformational changes upon lowering the pH (Fig. 1D). Repulsive interactions between the two origami sheets are expected to restrict these conformational changes to their x-plane movement rather than to a "closed" book state associated with the known and numerously demonstrated i-motif solution configuration<sup>18</sup> (Fig. 1D). Here, this pH-induced nanomechanical switching was electrochemically interrogated in order to establish the electronic principle of the nanomechanical event detection, which is particularly important for the design and exploitation of stimuli-responsive, surface-confined nanoscale electro-mechanical systems. Electrochemical detection could eventually be used to

<sup>&</sup>lt;sup>a</sup> Interdisciplinary Nanoscience Center (iNANO), Science and Technology, Aarhus University, Gustav Wieds Vej 14, 8000 Aarhus C, Denmark. E-mail: elena.ferapontova@inano.au.dk

<sup>&</sup>lt;sup>b</sup> Center for DNA Nanotechnology (CDNA) at iNANO, Science and Technology, Aarhus University, Gustav Wieds Vej 14, 8000 Aarhus C, Denmark

<sup>&</sup>lt;sup>c</sup> Department of Materials Science and Engineering, North Carolina State University, Raleigh, NC 27606, USA

<sup>†</sup> Electronic supplementary information (ESI) available: Experimental details, origami sequences/gel, and additional voltammetry/capacitance data. See DOI:

Communication ChemComm

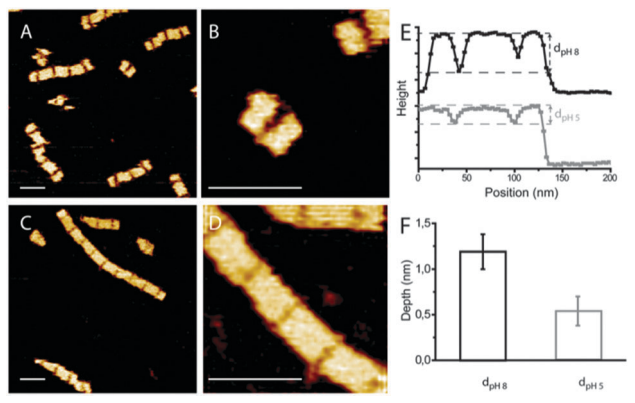


Fig. 2 (A-D) Representative AFM topographical images of queues of "open-book" i-motif origami in (A and B) pH 8 and (C and D) pH 5 imaging buffer solutions. The scale bar is 100 nm. In (C and D) the origami were kept at pH 5 for more than 30 min prior to adsorption on mica. (E) Typical line-profiles along the long-axis of the i-motif origami at pH 8 and 5. The height difference between the dashed lines indicates the AFM probe detected depth of the cleft between the two origami sheets at each pH value. (F) The distributions of the AFM detected depth of the i-motif gap at pH 8 and 5 averaged over 20 individual measurements. In (E and F), all experimental conditions are the same as in (A-D).

monitor conformational switching in novel sensing DNA nanostructures employing aptamers that change shape in response to specific ligand binding19 or redox-cascade reactions in enzymemodified DNA origami scaffolds.20

On atomically flat hydrophilic mica (the conventional substrate for origami visualisation), in the presence of the essential concentration of bivalent cations (ESI†), well-resolved "open book" origami structures were observed by AFM with a nanoscale resolution (Fig. 2A and B). Those structures were composed either of one (Fig. 2B) or few origami structures stuck together linearly by bluntend helix stacking12 (Fig. 2A and 3A), in which central open i-motif regions could be seen (Fig. 2A and B). With decreasing pH, the i-motif sequences fold into quadruplex structures, resulting in the origami's i-motif compact cleft state (Fig. 2C and D). DNA with low packing density is a true challenge for detection by AFM, a single stranded DNA (such as the i-motif region) being an extreme case.<sup>21</sup> Hence, at pH 8, the measured height of the i-motif region in the "open book" state is much lower than that of the DNA-origami sheets (Fig. 1B and D, panel a); and the height difference is marked as  $d_{\rm pH-8}$  (Fig. 2E). At pH 5, under the similar imaging force, the height difference between the DNA-origami sheets and the i-motif region ( $d_{\text{pH-5}}$ ) decreased more than two-fold compared to  $d_{\text{pH-8}}$ (Fig. 2E and F), consistent with compaction of the cleft at low pH. We believe that the formation of the i-motif quadruplex structures does actually decrease the cleft depth and, in return, diminish the cleft size, as a result of the increasing local packing strength between the two DNA origami "book" sheets.

Importantly, those conformational changes stemming from the nanomechanical movements of the i-motif origami are inconsistent with a pH-induced transition of the "open-book" to the "closed-book" state (Fig. 1D, panel c); no "closed-book" structures being detected for DNA origami deposited from pH 5 solutions. On surfaces, the pH-induced planar movement of the

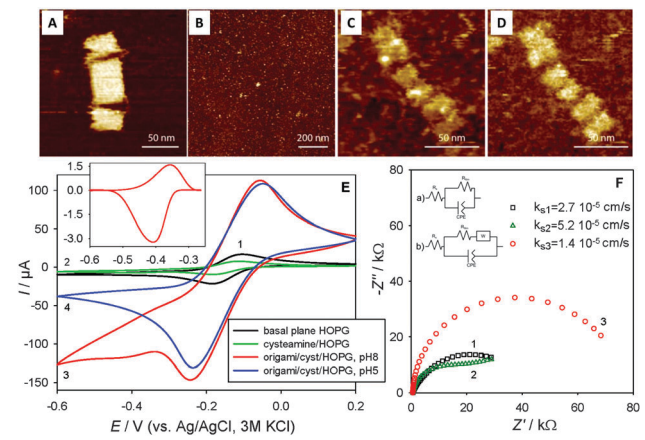


Fig. 3 (A-D) AFM images of DNA origami in TAE/Mg<sup>2+</sup> buffer, pH 8.0, on (A) mica, (B) HOPG, and (C and D) cysteamine-modified HOPG; (D) is the AFM phase image of (C). (E) Representative cyclic voltammograms recorded in 1 mM Ru(NH<sub>3</sub>)<sub>6</sub><sup>3+</sup>-containing TAE/Mg<sup>2+</sup> buffer solutions: (1) bare HOPG, (2) cysteamine-modified HOPG, (3 and 4) cysteamine-modified HOPG after assembly of 50  $\mu$ L of 15 nM DNA origami, (1–3) pH 8, (4) pH 5. The potential scan rate is 50 mV s<sup>-1</sup>. Inset: background-corrected Ru(NH<sub>3</sub>)<sub>6</sub><sup>3+</sup> adsorption peaks from (3). (F) Representative electrochemical impedance spectra (EIS) recorded in 2 mM Fe(CN)<sub>6</sub><sup>3-/4-</sup>-containing TAE/Mg<sup>2+</sup> buffer solution, pH 8.0, at E = 0.25 V. In (1-3) modification conditions are the same as in (E). Insets: the equivalent circuits used to fit the EIS data, (a) for (1; 3) and (b) for (2); and the apparent ET rate constants for those modifications calculated from the charge transfer resistance data,  $R_{ct}^{33}$  (ESI†).

two "open-book" origami planes, driven toward one another by the folding of the i-motif structures, is clearly detected (Fig. 2D, panels a and b).

No origami assemblies were observed on the unmodified basal plane HOPG surface, consistent with previous reports<sup>22</sup> (Fig. 3B). The electrochemical response from  $Ru(NH_3)_6^{3+}$ , a redox indicator known to specifically interact with surfaceimmobilised DNA11,23,24 was quite similar before and after bare HOPG exposure to DNA (Fig. S2, ESI†).

For DNA origami assembling on such conductive support as the atomically flat and hydrophobic basal plane HOPG, widely used for AFM imaging and electrochemical studies of nm scale objects, 25-27 an extra surface modification is required. Therewith, the surface charge and properties should promote intact origami adsorption, otherwise it can result in either DNA unfolding or interaction directly through the bases.<sup>22,28</sup> While there are several reports on DNA imaging on HOPG modified with a self-polymerised film, 29,30 the unknown composition of the film excludes its broader applications. An alternative method is light-assisted chemisorption of functionalised alkanethiols<sup>22</sup> bearing positively charged amine groups (-NH<sub>2</sub><sup>+</sup>) that may promote surface adsorption of the negatively charged DNA origami assemblies.

Here, the freshly cleaved basal plane HOPG surface was modified with cysteamine following reported protocols,<sup>31</sup> by its surface irradiation in O2-free DMF solution containing H2O and cysteamine (see ESI† for details). On the positively-charged modified HOPG surface (cysteamine  $pK_a$  of 10.73<sup>32</sup>), the electrochemical signal from Ru(NH<sub>3</sub>)<sub>6</sub><sup>3+</sup> decreased 20% due to Ru(NH<sub>3</sub>)<sub>6</sub><sup>3+</sup> electrostatic repulsion (curves 1 and 2, Fig. 3F). In contrast, the

ChemComm Communication

electron transfer (ET) reaction of the anionic redox indicator  $\operatorname{Fe}(\operatorname{CN})_6^{3-/4-}$  at positively-charged HOPG surface was improved as evidenced by the decreased charge transfer resistance,  $R_{\rm ct}$ , and the correspondingly increased ET rate constant,  $k_{\rm s(i)}$  (Fig. 3F and Table S1, ESI†).

When DNA origami was deposited onto the cysteamine-modified HOPG surface (Fig. 3C and D), a dramatic increase in the voltammetric signal from Ru(NH<sub>3</sub>)<sub>6</sub><sup>3+</sup> (curve 3, Fig. 3E) and the  $R_{\rm ct}$  increased from 20 to 74 k $\Omega$ , associated with the decrease in the  $k_{\rm s(i)}$  for Fe(CN)<sub>6</sub><sup>3-/4-</sup> was observed (Fig. 2F and Table S1, ESI†), consistent with the immobilisation of the DNA origami onto the modified HOPG.

 ${\rm Ru(NH_3)_6}^{3^+}$  is known to electrostatically interact with the negatively-charged sugar–phosphate backbone of DNA<sup>34</sup> and can form conductive wires along the DNA strands,<sup>11</sup> while the  ${\rm Fe(CN)_6}^{3^-/4^-}$  couple is electrostatically repelled by the backbone and exhibits a typical diffusion-limited ET behaviour.<sup>35,36</sup> The increase in the  ${\rm Ru(NH_3)_6}^{3^+}$  signal intensity on the DNA origami-modified HOPG (diffusion-limited peaks at  $-149 \pm 11$  mV, the peak currents changing linearly with the square root of the potential scan rate<sup>37</sup>) is then associated with the attractive electrostatic interactions between the DNA origami and  ${\rm Ru(NH_3)_6}^{3^+}$ , while electrochemistry of  ${\rm Fe(CN)_6}^{3^-/4^-}$  was electro-statically impeded by the origami assemblies. It is important that independently of the potential applied, the origami assembly was stable at the electrode surface both with positive and negative charging of the electrode (the HOPG potential of zero charge of -0.1 V, Fig. S3, ESI†).

Along with that, a characteristic Ru(NH<sub>3</sub>)<sub>6</sub><sup>3+</sup>-DNA adsorption peak at  $-390 \pm 20$  mV (the peak currents linearly proportional to the scan rate<sup>37</sup>) evidenced the formation of the Ru(NH<sub>3</sub>)<sub>6</sub><sup>3+</sup> wire bridges along the DNA structures. No adsorption peaks to be correlated with the electronic wire formation were detected for double stranded DNA and four-way DNA Holiday Junctions<sup>4</sup> adsorbed onto the modified HOPG surface (Fig. S4B and C, ESI†). Similar adsorption peaks were earlier reported for short, doublestranded DNA vertically oriented on the electrode surface<sup>11,24</sup> (Fig. S4A, ESI†) and for G4 structures, 38 although at less negative potentials ( $-264 \pm 20$  mV). The peak potential difference is apparently associated with a higher negative charge localised on the tightly packed DNA origami nanostructures, producing corresponding changes in the electric double layer potential distribution. <sup>39,40</sup> Therewith, formation of the Ru(NH<sub>3</sub>)<sub>6</sub> <sup>3+</sup> wire should occur within the i-motif region, more flexible than other origami regions and oriented vertically towards the electrode surface, along with that providing an immediate surface contact between the electrode and Ru(NH<sub>3</sub>)<sub>6</sub><sup>3+</sup> decorating the DNA origami. That appears to be sufficient to produce the electronic wire effect.

The rate constant,  $k_{\rm s}$ , for ET between HOPG and DNA-bound Ru(NH<sub>3</sub>)<sub>6</sub><sup>3+</sup>, was 1.3  $\pm$  0.2 s<sup>-1</sup>, which is rather comparable to the  $k_{\rm s}$  for ET reactions of methylene blue or anthraquinone bound to DNA duplexes (1.9 and 1.3 s<sup>-1</sup>, correspondingly), not to that of the Ru(NH<sub>3</sub>)<sub>6</sub><sup>3+</sup> wires (321 s<sup>-1</sup> for  $\Gamma_{\rm DNA}$  = 3.0 pmol cm<sup>-2</sup>).<sup>11,24</sup> Ru(NH<sub>3</sub>)<sub>6</sub><sup>3+</sup> binding to DNA origami appears to differ from the ideal one-dimensional conductor,<sup>11</sup> which actually can be anticipated considering strong effects of the interfacial structure and DNA packing on the mechanism of ET reactions of DNA-bound species.<sup>24</sup>

The pH-induced i-motif nanomechanical switching at the HOPG surface was electrochemically read-out by following the variation of the signal from the Ru(NH<sub>3</sub>)<sub>6</sub><sup>3+</sup> adsorption within the i-motif region. In acidic solutions, the i-motif "open book" switched to the compact cleft structure, with the i-motif region now tighter packed due to its folding into quadruplex. This resulted in the disappearance of the adsorption peaks detected in basic solutions, while the Ru(NH<sub>3</sub>)<sub>6</sub><sup>3+</sup> diffusional signals remained practically the same, indicating the presence of origami immobilized at the electrode surface (curves (3-4), Fig. 3E). It follows from these data that the origami remained integrated at the electrode surface. However, in contrast to mica, the AFM imaging of the origami state at HOPG was not of a sufficiently high resolution to visualise the origami conformational state at pH 5. Along with that, those variations were directly readout electrochemically.

In conclusion, i-motif DNA origami was self-assembled onto conductive cysteamine-modified basal plane HOPG surface and these origami assemblies were shown to be stable under applied electric fields, both at negative and positive charging of the electrode surface. The pH-induced conformational nanomechanical switching of the DNA origami was accomplished both on mica and modified HOPG, on the latter it was electronically addressed by following electrochemical signals from the redox indicator specifically interacting with the pH-switchable i-motif origami region. Demonstrated electronically controllable nanoswitching of complex DNA origami nanostructures at electrodes paves the way for design and further construction of bioelectronically addressable electrode integrated nanomechanical devices exploiting DNA origami patterns.

The work was supported by the Danish National Research Foundation (DNRF) through their support to the CDNA, grant number DNRF81, and by the US National Science Foundation grant EPMD-1231888. We acknowledge CAPES and CNPq for a Science Without Borders Scholarship which permitted L. C. C. Ferraz to collaborate on this project.

## Notes and references

- 1 Z. Jin, W. Sun, Y. Ke, C. J. Shih, G. L. C. Paulus, Q. H. Wang, B. Mu, P. Yin and M. S. Strano, *Nat. Commun.*, 2013, 4, 1663.
- 2 S. M. Douglas, I. Bachelet and G. M. A. Church, *Science*, 2012, 335, 831–834.
- 3 N. A. W. Bell, C. R. Engst, M. Ablay, G. Divitini, C. Ducati, T. Liedl and U. F. Keyser, *Nano Lett.*, 2012, 12, 512–517.
- 4 E. E. Ferapontova, C. P. Mountford, J. Crain, A. H. Buck, P. Dickinson, J. S. Beattie, P. Ghazal, J. G. Terry, A. J. Walton and A. R. Mount, *Biosens. Bioelectron.*, 2008, 24, 422–428.
- 5 H. Yan, X. P. Zhang, Z. Y. Shen and N. C. Seeman, *Nature*, 2002, 415, 62–65.
- 6 H. Liu and D. S. Liu, Chem. Commun., 2009, 2625-2636.
- 7 Y. Krishnan and F. C. Simmel, Angew. Chem., Int. Ed., 2011, 50, 3124-3156.
- 8 O. I. Wilner and I. Willner, Chem. Rev., 2012, 112, 2528-2556.
- 9 E. Braun, Y. Eichen, U. Sivan and G. Ben-Yoseph, *Nature*, 1998, 391, 775–778
- 10 W. Kaiser and U. Rant, J. Am. Chem. Soc., 2010, 132, 7935-7945.
- 11 A. Abi and E. E. Ferapontova, J. Am. Chem. Soc., 2012, 134, 14499–14507.
- 12 P. W. K. Rothemund, Nature, 2006, 440, 297-302.
- 13 J. M. Majikes, L. C. C. Ferraz and T. H. LaBean, 2015, submitted.

- Communication ChemComm
- 14 S. Brown, J. M. Majikes, A. Martínez, T. M. Girón, H. Fennell, E. C. Samano and T. H. LaBean, 2015, submitted.
- 15 A. L. Lieblein, J. Buck, K. Schlepckow, B. Furtig and H. Schwalbe, Angew. Chem., Int. Ed., 2012, 51, 250–253.
- 16 C. H. Kang, I. Berger, C. Lockshin, R. Ratliff, R. Moyzis and A. Rich, Proc. Natl. Acad. Sci. U. S. A., 1995, 92, 3874–3878.
- 17 N. Escaja, J. Viladoms, M. Garavis, A. Villasante, E. Pedroso and C. Gonzalez, *Nucleic Acids Res.*, 2012, 40, 11737–11747.
- 18 Y. C. Dong, Z. Q. Yang and D. S. Liu, Acc. Chem. Res., 2014, 47, 1853–1860.
- 19 E. J. Cho, J.-W. Lee and A. D. Ellington, Annu. Rev. Anal. Chem., 2009, 2, 241–264.
- 20 C. Timm and C. M. Niemeyer, Angew. Chem., Int. Ed., 2015, 54, 6745–6750.
- 21 J. Song, Z. Zhang, S. Zhang, L. Liu, Q. Li, E. Xie, K. V. Gothelf,
- F. Besenbacher and M. Dong, *Small*, 2013, 9, 2954–2959.
  D. Alloyeau, B. Q. Ding, Q. Ramasse, C. Kisielowski, Z. Lee and K. J. Jeon, *Chem. Commun.*, 2011, 47, 9375–9377.
- 23 A. B. Steel, T. M. Herne and M. J. Tarlov, *Anal. Chem.*, 1998, 70, 4670-4677
- 24 R. Campos and E. E. Ferapontova, Electrochim. Acta, 2014, 126, 151-157.
- 25 C. R. Bradbury, L. Kuster and D. J. Fermin, J. Electroanal. Chem., 2010, 646, 114–123.
- 26 M. Tanaka, T. Sawaguchi, Y. Sato, K. Yoshioka and O. Niwa, *Langmuir*, 2011, 27, 170–178.

- 27 P. Lopes, M. Xu, M. Zhang, T. Zhou, Y. L. Yang, C. Wang and E. E. Ferapontova, *Nanoscale*, 2014, 6, 7853–7857.
- 28 B. Song, D. Li, W. P. Qi, M. Elstner, C. H. Fan and H. P. Fang, ChemPhysChem, 2010, 11, 585-589.
- 29 D. Klinov, B. Dwir, E. Capon, N. Borovok, T. Molotsky and A. Kotlyar, Nanotechnology, 2007, 18, 225102.
- 30 D. Klinov, B. Dwir, E. Kapon, N. Borovok, T. Molotsky and A. Kotlyar, AIP Conf. Proc., 2006, 859, 99–106.
- 31 L. Soldi, R. J. Cullen, D. R. Jayasundara, E. M. Scanlan, S. Giordani and P. E. Colavita, J. Phys. Chem. C, 2011, 115, 10196–10204.
- 32 D. C. Harris, *Quantitative Chemical Analysis*, W. H. Freeman & Co Ltd, New York, 5th edn, 1999.
- 33 E. Ferapontova and K. V. Gothelf, Langmuir, 2009, 25, 4279-4283.
- 34 A. B. Steel, T. M. Herne and M. J. Tarlov, *Bioconjugate Chem.*, 1999, 10, 419–423.
- 35 E. E. Ferapontova, Curr. Anal. Chem., 2011, 7, 51-62.
- 36 A. Abi, M. H. Lin, H. Pei, C. H. Fan, E. E. Ferapontova and X. L. Zuo, ACS Appl. Mater. Interfaces, 2014, 6, 8928–8931.
- 37 A. Bard and L. Faulkner, Electrochemical Methods: Fundamentals and Applications, John Wiley & Sons, 2001.
- 38 A. De Rache, T. Doneux and C. Buess-Herman, Anal. Chem., 2014, 86, 8057–8065.
- 39 E. E. Ferapontova and N. V. Fedorovich, J. Electroanal. Chem., 1999, 476, 26–36.
- 40 E. E. Ferapontova, J. Electroanal. Chem., 1999, 476, 37-45.